TU3E-(SS1)-3

EFFECTS OF THERMAL ANNEALING ON InGaN/GaN QUANTUM WELL STRUCTURES WITH SILICON DOPING

Yung-Chen Cheng, En-Chiang Lin, Shih-Wei Feng, Hsiang-Chen Wang, and C. C. Yang
Graduate Institute of Electro-Optical Engineering, Graduate Institute of Electronics Engineering and Department of Electrical Engineering,
National Taiwan University, 1, Roosevelt Road, Sec. 4, Taipei, Taiwan, R.O.C.
(phone) 886-2-23657624 (fax) 886-2-23652637 (E-mail) ccy@cc.ee.ntu.edu.tw
Kung-Jen Ma
Department of Mechanical Engineering, Chung Hua University, Hsinchu, Taiwan, R.O.C.
Shih-Chen Shi and L. C. Chen
Center for Condensed Matter Sciences, National Taiwan University, Taipei, Taiwan, R.O.C.
Chang-Chi Pan and Jen-Inn Chyi
Department of Electrical Engineering, National Central University, Chung-Li, Taiwan, R.O.C.

Abstract: *The effects of thermal annealing on the optical properties and material structures of InGaN/GaN quantum wells with silicon doping were studied to find that the material microstructures alternation was the major reason for the changes.*

Silicon-doped InGaN/GaN quantum wells (QWs) have attracted lots of interest because of the improved photon emission efficiency. The improvement with silicon doping was attributed to the screening of piezoelectric fields. Because high temperature growth of a GaN upper cladding layer on top of the QWs is needed for fabricating light-emitting devices, a thermal annealing procedure on the QWs is inevitable. Therefore, the study of the post-growth thermal annealing effects on InGaN/GaN QWs with silicon doping is very important for improving the efficiency of a related light-emitting device. The sample consisted of five QW periods with ~2.5 nm in well width and ~7.5 nm in barrier width on top of the un-doped GaN buffer layers with thickness 1.52 μm. The barrier doping concentration is 5 x 10^{18} cm^{-3}. The as-grown, thermal annealing at 700 °C for 15 min, and 800 °C for 30 min samples were referred to as samples A, B, and C, respectively. Figure 1 shows the PL and PLE spectra of the as-grown and post-thermal annealing samples at 10K. One can see that the Stokes shifts (SSs) are around 500 meV for the three samples. Figure 2 shows the Arrhenius plots of temperature-dependent integrated intensity of the three samples. The solid lines represent the best-fitting curves by using the equation $I(T)=A_0(1+B_0\exp(-E_{A1}/kT)+C_0\exp(-E_{A2}/kT))^{-1}$. $I(T)$ is the temperature-dependent normalized integrated PL intensity. The two activation energies E_{A1} and E_{A2} correspond to two different decay processes. The notations B_0 and C_0 represent the ratios of the probability of non-radiative to that of radiative transitions. The large increase of C_0 of sample C was obserevd. The values of the activation energies E_{A2} are around 65meV. The formed indium-rich clusters along the QWs can be seen in the as-grown sample A. In sample C, the designated QWs become widely dispersed. In CL images, large areas of bright spots can be seen in sample A. However, such large bright spots became smaller with annealing at 800 °C for 30 min. The Stokes shift and high-temperature-related activation energy E_{A2} are related to the built-in piezoelectric fields and carrier localization in potential minima. As previously reported, piezoelectric fields are expected small in barrier-doped InGaN/GaN QW structures. The small changes in SS and activation energies E_{A2} upon thermal annealing indicate that the strains and potential fluctuations are not strongly affected by thermal annealing under the two annealing conditions. From the HRTEM results of sample C, the increase of non-radiative recombination centers can originate from the increase of defect density. Also, it can be attributed to the weaker carrier localization due to microstructure variation upon thermal annealing.

Fig. 1

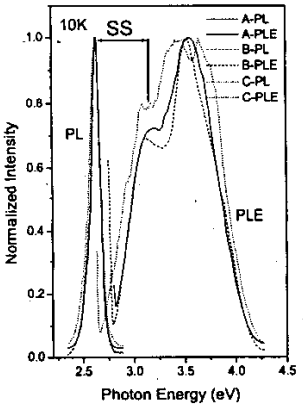

Fig. 2

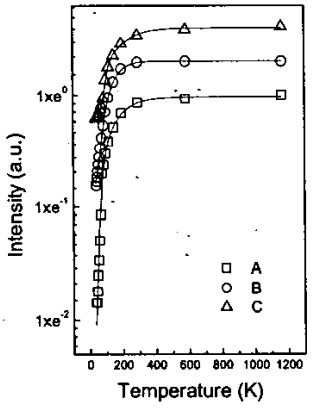

0-7803-7766-4/03/$17.00 ©2003 IEEE